JOURNAL OF OPTOELECTRONICS AND ADVANCED MATERIALS Vol. 9, No. 6, June 2007, p. 1736 - 1741

Synthesis and properties of some Nd-Sr manganites dopped with indium

M.-L. CRAUS[a,b], N. CORNEI[c]
[a]*FLNP- Joint Institute for Nuclear Research, Joliot-Curie 6, 141980 Dubna, Russia*
[b]*National Institute of Research and Development for Technical Physics, D. Mangeron 47, Iassy, Romania*
[c]*"Al.I.Cuza" University, Carol I 6, Iassy Romania*

We have synthesized magnetoresistive bulk manganites by sol-gel technology. The synthesis method started from a homogeneous aqueous solution consisting of the metal ions and chelating or bridging ligands. The proof of the chemical composition and the $Mn^{3+}Mn^{4+}$ concentrations ratio were obtained by means of EDX and, respectively, van Santen methods. The sintered samples were also investigated by means of electron microscopy and XRD; lattice constants, space group, position of cations/anions in the unit cell, average size of the crystalline blocks and microstrains were obtained with TREOR, CechCell and FullProf programs. The variation of the specific/molar magnetization with the temperature was determined by using Foner –type magnetometer, between 77 and 550 K. The electric measurements were made by using a four-probe device. We found that the unit cell type and lattice parameters strongly depend on the (Nd, In) /Sr concentration and the sintering conditions. The extrinsic effects caused by the distorted boundaries layers of the crystallites, on the hand, and the (Nd, In)/Sr concentrations ratio, on other hand, rule over the transport behavior. The substitution of Nd with In seems to move the ferromagnetic metallic region of the $(Nd_{0.67}In_{0.33})_{1-x}Sr_xMnO_3$ at lower Sr concentrations as compared with $Nd_{1-x}Sr_xMnO_3$ system.

(Received November 14, 2006; accepted April 26, 2007)

Keywords: Magnetoresistance, Crystalline and magnetic structure, Nd-Sr manganites

1. Introduction

The $Alk_{1-x}Re_xMnO_3$ manganites (Alk=Sr, Ba, Ca; Re=rare earth) are electronic materials of considerable interest. Some manganites exhibit a large magnetoresistance at room temperature. The transport properties were explained in the terms of Zener double exchange theory [1], which consider the transfer of e^g electrons of Mn^{3+} to Mn^{4+} cations via O2p orbitals. At temperatures higher as those corresponding to transition from ferromagnetic to paramagnetic state, manganites exhibit a dependence of resistivity on magnetic field intensity. Meneghini et al supposed that in paramagnetic region the transport mechanism is dominated by a strong electron-lattice interaction [2]. The $Mn^{3+}Mn^{4+}$ concentrations ratio is determined by the Alk/Re concentrations ratio and the oxygen concentration of the manganites. The change of the Mn^{3+} concentration leads to a modification of the electronic phase composition and of the crystalline structure of the manganites. The magnetoresistance have two components: 1)intrinsic magnetoresistance, which varies at $T<T_C$ like $\sim[1-(M/M_s)^2]$ [3] or on the logarithmic law $\ln\rho\sim - M/M_s$ [4] and 2)extrinsic magnetoresistance, which is due to the charges scattering on the boundary layers of the crystallites or on the boundary of magnetic domains. At temperatures higher as Curie temperature were proposed more charge transport models:
1) semiconductor – like:

$$\rho = \rho_0 \exp\left(\frac{E_a}{kT}\right) \quad (1)$$

2) variable range hopping [5]:

$$\rho = \rho_\infty \exp\left[\left(\frac{T_0}{T}\right)^m\right] \quad (2)$$

3) small polaron hopping [6]:

$$\rho = \rho_P T \exp\left(\frac{E_p}{kT}\right) \quad (3)$$

where the activation energies (E_a, E_p) of the processes depend on the C_{Mn3+}/C_{Mn4+} and C_{Alk}/C_{Re} ratios (C_{Mn3+} represents the amount of Mn^{3+} cations on the formula unit etc).

The structure of manganites is governed by the tolerance factor (t). The perovskite structure is stable for $0.89<t<1.02$, $t=1$ corresponding to the perfect cubic structure. Real manganites have a tetragonal, rhombohedral or orthorhombic structure. The $(Alk, Re)_{1-x}Sr_xMnO_3$ with $x<0.5$ have a hole conduction, while $x>0.5$ have an electron conduction. The increase of the x over 0.5 lead to a decrease of the DE links, implicitly to an increase of AF coupled Mn^{4+} cations.

Our aims are to investigate the influence of the synthesis conditions on the electronic/crystalline phase composition, the magnetic structure and the extrinsic magnetoresistance in the $(Nd_{0.67}In_{0.33})_{1-x}Sr_xMnO_3$ manganites.

2. Experimental

Manganites with $(Nd_{0.67}In_{0.33})_{1-x}Sr_xMnO_3$ nominal composition were synthesized by sol-gel method and finally sintered at 1300 °C. The details concerning the sol-gel method and the determination of C_{Mn3+}/C_{Mn4+} ratio was presented in [7]. The sintered samples were investigated by X-ray diffraction (XRD) by using a STOE (Guinier type) diffractometer (Cu Kα monochromatized radiation). Lattice constants and space group were determined and tested by using TREOR, DICVOL and, respectively, CheckCell programs [8, 9, 10]. The positions of the atoms in the unit cell were determined by means of Powder Cell programe [11]. Calculated and observed tolerance factors were determined with relations:

$$t_{calc} = \frac{\langle r_A \rangle + r_O}{\sqrt{2}(\langle r_B \rangle + r_O)} \quad (4)$$

$$t_{obs} = \frac{\langle d_{A-O} \rangle}{\sqrt{2}\langle d_{Mn-O} \rangle} \quad (5)$$

due to Jonker [12]. Chemical disorder factor, η, were determined with formula[13]:

$$\eta^2 = \sum_i C_i r_i^2 - \langle r_A \rangle^2 \quad (6)$$

where C_i and r_i is the concentration and, respectively, radius of the i atom.

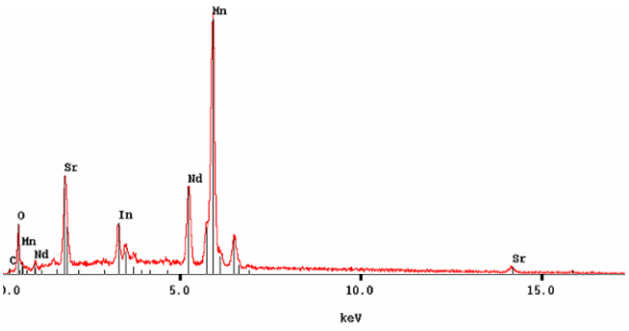

Fig. 1. The EDX of the $Nd_{0.54}In_{0.26}Sr_{0.2}MnO_3$.

Because the extrinsic magnetoresistance strongly depend on the crystalline defaults, we determined also the average size of the crystalline blocks and the microstrains.

The band width was calculated with the relation:

$$w \propto \frac{\cos(\angle Mn - O - Mn)}{(d_{Mn-O})^{3.5}} \quad (7)$$

The chemical composition of the sintered manganites was obtained by EDX (s. Fig. 1), the results confirming the previewed ratio between the cation concentrations. The variation of the specific magnetization/molar magnetization (σ/p) with the temperature, Curie temperature (T_C) were determined by using a Foner type magnetometer, previewed with acquisition data system, between 77 and 550 K. The system was calibrated by using a Ni sphere (Erba, Italy). The electrical measurements were performed using the four-probe device, previewed with acquisition data system.

3. Results and discussion

All sintered $(Nd_{0.67}In_{0.33})_{1-x}Sr_xMnO_3$ manganites (x=0.2, 0.35, 0.5, 0.65) contain a main phase, which can be considered an orthorhombic distorted tetragonal structure. By means of CheckCell and PowderCell programs we found that the most suitable space group associated with the main phase of sintered at 1300 °C manganites is Pnma (GS 62). Small concentration of In_2O_3 (less as 5%) was evidenced by XRD (see Fig. 2).

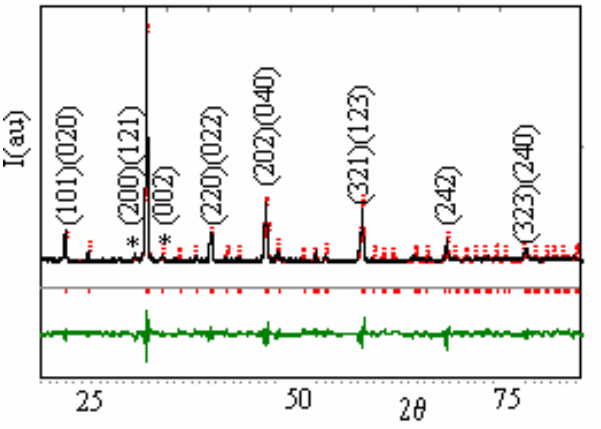

Fig. 2. Observed and calculated diffractograms of $Nd_{0.54}In_{0.26}Sr_{0.2}MnO_3$ manganite. The asterisk (*) indicates the maxima of In_2O_3.

Due increasing the sintering temperature, the samples contain a smaller oxygen concentration, implicitly a smaller amount of Mn^{4+} concentration.

The increase of the Sr concentration in the samples leads to an decrease of a/c lattice constants ratio (s.Tab.1), an increase of the microstrains (ε) (s.Tab.2) and of the unit cell volume (s.Tab.3). The average size of the crystalline blocks (D) remain practically constant for x=0.2 and x=0.35, but attains a minimum and a maximum value for x=0.35 and, respectively, for x=0.65 (s.Tab.2).

Table 1. Lattice constants (a, b, c) of $(Nd_{0.67}In_{0.33})_{1-x}Sr_xMnO_3$ manganites.

x	a(Å)	b(Å)	c(Å)	a/c	b/a
0.20	5.485_5	7.690_1	5.425_1	1.01_1	1.40_2
0.35	5.489_8	7.691_9	5.450_4	1.00_7	1.40_1
0.50	5.447_0	7.748_2	5.445_6	1.00_0	1.42_2
0.65	5.476_3	7.745_5	5.538_4	0.98_9	1.41_4

The sample corresponding to x=0.50 is practically tetragonal ($a \approx c < b/\sqrt{2}$) (Table 1), while for those corresponding to x=0.65 we can consider a tetragonal structure with $a \approx c' = b/\sqrt{2}$ (Table 1). The increase of the unit cell volume is in agreement with the A cation radii

(r_{In3+}=0.120; r_{Nd3+}=0.127; r_{Sr2+}=0.144 nm) (crystalline radii on Shannon).

Table 2. Atomic positions (x, y,z) in the unit cell, average size of the crystalline blocks (D) and microstrains (ε) of $(Nd_{0.67}In_{0.33})_{1-x}Sr_xMnO_3$ manganites.

x→ Coordina ↓	0.20	0.35	0.50	0.65
$x_{Nd,In,Sr}$	0.0426	0.0218	0.0161	0.0169
$z_{Nd,In,Sr}$	0.0054	0.0101	0.0110	0.0108
$x_{O1,ap}$	0.4771	0.4829	0.4804	0.4802
$z_{O1,ap}$	0.0572	0.0572	0.0320	0.0318
$x_{O2,eq}$	0.2819	0.2821	0.2937	0.2737
$y_{O2,eq}$	0.0371	0.0381	0.0571	0.0471
$z_{O2,eq}$	0.7270	0.7760	0.7483	0.7480
D (nm)	69.27	70.46	50.56	93.27
ε	0.00036	0.00046	0.00087	0.00170

The observed difference between the calculated and observed tolerance factor are attributed to a small difference between the nominal and real chemical composition of the manganites (s.Table 3) and to the decrease of the Mn^{3+} concentration in the samples. The presence of cations with different ionic radii size on A/B places, due to the caused by the mismatch between the average radius and the local radius of a place, play a significant role in the phase separation and transport properties of the manganites. The e_g electrons hopping rate depends on the exchange coupling constant, also determined by the crystallography of Mn-O-Mn bonds, implicitly, by the average radius of A places. Local variation in the exchange constant and $\langle r_A \rangle$ leads to the appearance of the local AF or FM states. It is known that an important feature of $(Nd_{0.67}In_{0.33})_{1-x}Sr_xMnO_3$ manganites is that the MnO_6 octhaedra consist of two short and one long O-Mn-O bonds for x≤0.35 and one short and two long O-Mn-O bonds, respectively, for x>0.35. In agreement with results of Kawano et al [14] we consider that the d_{x2-y2} type orbitals and, implicitly, the associated atomic magnetic moments lie within the (010) plane, for x>0.35. The moments of neighbor (010) planes are antiferromagnetic aligned. An important antiferromagnetic interaction between the two adjacent planes takes places even at the temperatures lower as Curie temperature. This manganites feature could enhance the appearance of the phase separation, at an increase of chemical disorder degree/decrease of tolerance factor.

Table 3. The calculated, observed tolerance factor (t_{calc}, t_{obs}), the disorder degree (η) and the unit cell volume (V)

x	t_{calc}*	t_{obs}	η	V(Å^3)
0.20	0.950	0.915	0.0117	229.992
0.35	0.972	0.958	0.0142	230.154
0.50	0.994	0.863	0.0145	230.435
0.65	1.017	0.889	0.0127	231.650

*)calculated by using the crystalline Shannon radii

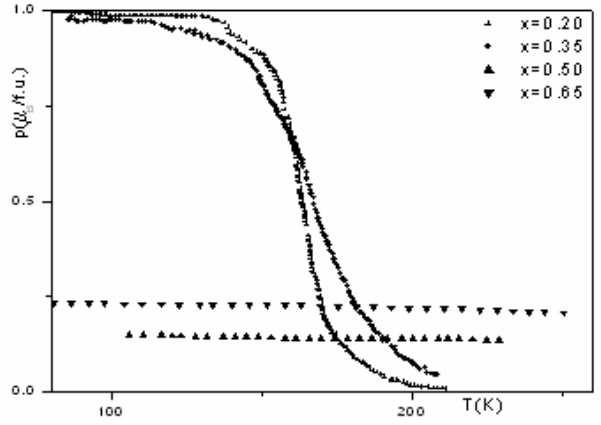

Fig. 3. Variation of the molar magnetization with the temperature and chemical composition.

For the samples with x<0.5 the increase of the t_{obs} and t_{calc} is associated with the increase of the Curie temperature, the decrease of the band width and of the observed molar magnetization (p_{obs}) (Table 4 and 5). The calculated molar magnetic moments have a maximum for x=0.5. The samples with x≥0.5 present a small magnetic moment, which remains almost constant with the temperature in the investigated range of temperatures (Fig. 3).

The decrease of the tolerance factor could lead to the appearance of the spin-glass state at low temperature. On other hand, the decrease of the tolerance factor and the increase of chemical disorder degree are associated with the decrease of T_C [13]. With the increase of the chemical disorder degree, the compound becomes inhomogeneous magnetically, this being the cause of the appearance of SGI state.

The magnetism in manganites is due to an interplay between the double exchange and superexchange interaction [7,15]. The t_{2g} Mn electrons are strongly correlated, even in the metallic state [15]. The metallic behavior of the manganites is due to the double exchange, associated with the overlap of e_g Mn and $2p_\sigma$ O orbitals. The crystallographic data suggest the appearance of an anisotropy of DE and SE interactions, with the increase of Sr concentration. The observed magnetic structure of manganites is due to a strong Hund coupling between the e_g and t_{2g} electrons. A competition between antiferromagnetic interaction and double exchange interaction takes place in manganites. The disappearance of the magnetic moment for the samples with x≥0.5 is in agreement with the observed tolerance factor (s.Tab.3). The calculated and observed magnetic moments attain a maximum, respectively, a minimum for x=0.5. The average d_{Mn-O} distances and ∠Mn-O-Mn angles have a maximum, respectively, a minimum for x≈0.35, on [001] direction. The band width, calculated with (7), behaves a strong directional anisotropy, being larger for [001] direction as for (001) plane.

Table 4. The average Mn-O distances ($\langle d_{Mn-O} \rangle$), A-O distances ($\langle d_{A-O} \rangle$), angles of Mn-O-Mn bond ($\langle \angle Mn\text{-}O\text{-}Mn \rangle$) and the average band width ($\langle |w| \rangle$).

x	$\langle d_{Mn-O} \rangle$ (Å)	$\langle d_{A-O} \rangle$ (Å)	$\langle \angle Mn\text{-}O\text{-}Mn \rangle$ (^{o})	$\langle \|w\| \rangle$ (a.u.)
0.20	1.9606	2.5359	159.674	0.081
0.35	1.9619	2.5288	159.439	0.067
0.50	1.9826	2.4150	154.243	0.087
0.65	1.9621	2.4673	161.318	0.043

The increase of the sintering temperature leads to a decrease of the molecular magnetic moment (s. ref. [7] and Table 4), due the decrease of the oxygen concentration in the sample. In agreement with ref [6], the introduction of oxygen defects strongly suppressed the Curie temperature (s. ref. [7] and Table 5). The increase of the bandwidth is associated with a decrease of T_C, in agreement with our data for x≤0.35 (Table 4 and 5).

Table 5. The observed and calculated molar magnetization (p_{obs}, p_{calc}) and the Curie temperature (T_C).

x	$p_{obs}(\mu_B)$	$P_{calc}(\mu_B)$	T_C(K)
0.20	0.985	1.386	163
0.35	0.973	2.443	168
0.50	0.150	3.472	<77
0.65	0.232	2.422	<77

For x>0.35 the observed magnetic moment of the manganites becomes very small (s.Tab.5 and Fig. 3). We interpret this behavior in connection with recent results due to Yunoki et al [16]. They have theoretically demonstrated that in certain range of dopping, a phase separation takes place between the hole-poor AF region and hole-rich FM region. The ferromagnetic metallic state is energetically more favorable than the homogenous canted-spin state. If the density is not sufficient to cover the entire sample, the carriers concentrate into the droplets or strips, which become ferromagnetic in an antiferromagnetic matrix.

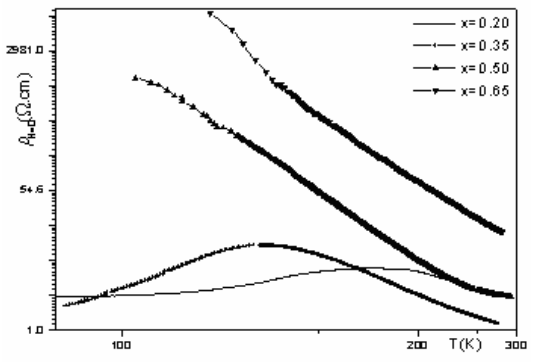

Fig. 4. The variation of resistivity with temperature and chemical composition.

In the actually investigated manganites the double exchange (DE)/superexchange (SE) interactions ratio is the result of 1) the variation of d_{Mn-O} distances of ∠Mn-O-Mn angles and 2) the variation of Mn^{3+}/Mn^{4+} concentrations ratio. For the samples with x>0.35 the SE interaction predominates, despite the presence of a large amount of Mn^{3+}-Mn^{4+} pairs.

The SE interactions is large enough to produces a canted-spin structure, not only in the samples with x>0.35, but also in the samples with x≤0.35. Comparing the calculated and observed molecular magnetic moment, we deduced that the angles between the spins of two neighbors Mn cations increase monotonously with Sr concentration (the magnetic structure, corresponding to x>0.35, are almost antiferromagnetic). The increase of the treatment temperature leads to a decrease of oxygen concentration in the samples and a corresponding decrease of the Mn^{3+}-Mn^{4+} pairs, as comparing with the same samples treated at 1200^{o}C [7]. It means also a decrease of DE interaction in the treated at 1300 ^{o}C $(Nd_{0.67}In_{0.33})_{1-x}Sr_xMnO_3$ manganites. Our results concerning the evolution of the magnetic state with the increase of Sr concentration are in agreement with the theory of spin –canting of Solovyev and Terakura on the $Re_{1-x}Alk_xMnO_3$ manganites [17]. On other hand, the appearance of a small magnetic moment at higher Sr concentration could be explained by the increases the magnetic disorder, implicitly with the formation of a non-homogenous magnetic state.

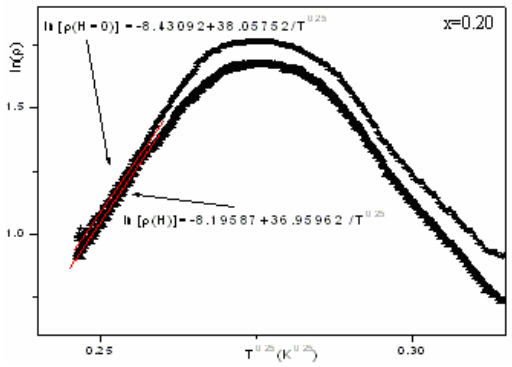

Fig. 5. Variation of resistivity with temperature and magnetic field intensity for the $Nd_{0.536}In_{0.264}Sr_{0.2}MnO_3$ manganite.

It is known that at temperatures higher as T_C, in the insulating state, the conductivity is due hopping of the lattice polarons, while below T_C the conductivity is the result of the movement of the individual electrons. In $Nd_{0.5}Sr_{0.5}MnO_3$ manganites the e_g holes and e_g electrons are itinerant at temperatures higher as T_C and localized below T_C [18]. For x<0.5 the manganites present a transition temperature (Fig. 5), which moves to lower temperatures with the increase of Sr concentration. For x≥0.5 the resistivity variation with the temperature has no maximum in the investigated range of temperatures (Fig. 6). Near transition temperature the dependence of

resistivity with temperature follow the Mott conduction law (s.Eq. (2), for m=1/4, and Fig. 5).

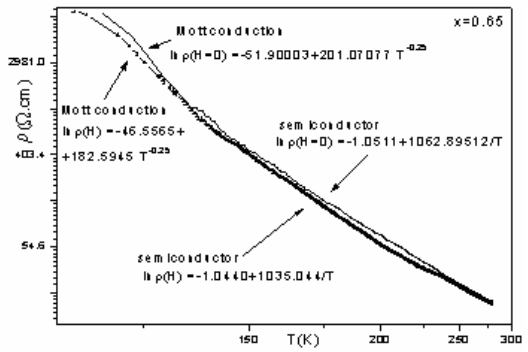

Fig. 6. Variation of the resistivity with the temperature and intensity of magnetic field for the $Nd_{0.234}In_{0.116}Sr_{0.65}MnO_3$ manganite.

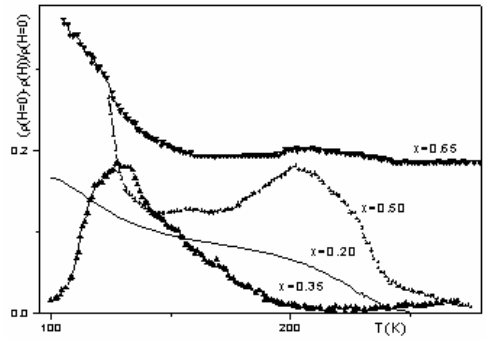

Fig. 7. variation of the magnetoresistance with the temperature and chemical composition for $(Nd_{0.67}In_{0.33})_{1-x}Sr_xMnO_3$ manganites

On the resistivity behavior with the temperature, a brake takes places for x>0.35: the transition temperature can be observed only for x≤0.35. A quasi metallic behavior was observed for these manganites at temperatures lower as transition temperature (s.Fig. 5). At the temperatures higher as transition temperature, for the samples with x≤0.35, and in the entire range of temperatures for the samples with x>0.35, we supposed that the transport mechanism can be described in the terms of variable range hopping mechanism (Figs. 5 and 6).

Despite the samples with x>0.35 exhibit no metallic behavior, a negative magnetoresistance was observed (Fig. 6).

The activation energies of the semiconductor type conduction decrease with the increase of Sr concentration and microstrains (Table 2 and 6).

Table 6. Activation energies (semiconductor range) and T_0 (VRH process constant) (s. Eq.(1) and (2)).

x	E_a(eV)		T_0(K)	
	H=0	H=2T	H=0	H=2T
0.20	-	-	2.10×10^6	1.87×10^6
0.35	-	-	1.29×10^7	0.89×10^7
0.50	0.101	0.102	1.90×10^8	1.78×10^8
0.65	0.092	0.090	1.64×10^9	1.11×10^9

Table 7. Radius of polaron (r_p) and the density of state at Fermi level ($N(E_F)$).

x	r_p (nm)		$N(E_F)(eV^{-1}.cm^{-1})$	
	H=0	H=2T	H=0	H=2T
0.20	0.449	0.467	7.2×10^{20}	6.4×10^{20}
0.35	0.245	0.277	4.4×10^{21}	3.1×10^{21}
0.50	0.100	0.102	6.5×10^{22}	$6.1*10^{22}$
0.65	0.049	0.056	5.7×10^{23}	$3.8*10^{23}$

Taking account that the average distance between cations is ≈ 0.226 nm, results that the VRH model is valid for x≥0.5. The obtained state density monotonously increases with the increase of Sr concentration in the samples (Table 7).

The magnetoresistance, near the room temperature, strongly depends on the defaults concentration in the samples (Fig. 7 and Table 2). For highest defaults concentration we observed a large component of the magnetoresistence, corresponding to x=0.65 (Fig. 7).

4. Conclusions

Variation of the oxygen or cation vacancies concentrations, due to the thermal treatment, induces variation of the magnetic properties, including the droplets concentration and their canted-spin magnetic structure.

The $(Nd_{0.67}In_{0.33})_{1-x}Sr_xMnO_3$ manganites with x>0.35 lie at the phase boundaries separating ferromagnetic and antiferromagnetic phases. The substitution of Nd with In and the increase of the treatment temperature lead to the increase of the disorder and the decrease of the tolerance factor, implicitly to the decrease of the Curie temperature and of the molar magnetic moment. The transport mechanism depends on the Sr concentration in $(Nd_{0.67}In_{0.33})_{1-x}Sr_xMnO_3$ manganites. The variable range hopping mechanism describes fairly well the transport charge behavior for the samples with x>0.35. Large defaults concentration, corresponding to x>0.35, leads to an increase of the (extrinsic) magnetoresistance.

References

[1] C. Zener, Phys. Rev. **82**, 403 (1951).
[2] C. Meneghini1, C. Castellano, S. Mobilio, A. Kumar, S. Ray, D. D. Sarma, J.P.:Cond. Matter **14**, 1967 (2002).
[3] Y. X. Jia, Li Lu, K. Khazeni, V. H. Crespi, A. Zettl, M. L.Cohen, Phys.Rev. **B52**, 9147 (1995).
[4] M. F. Hundley, J. J. Neumeier, R. H. Heffner, Q. X. Jia, X. D. Wu, J. D. Thompson, J. Appl. Phys. **79**, 4535 (1996).
[5] M. Paraskevopoulos, F. Mayr, J. Hemberger, A. Loidl, R. Heichele, D. Maurer, V. Mueller, A. A. Mukhin, A. M. Balbashov, J. Phys.: Condens. Matter. **12**, 3993 (2000).

[6] M. L. Wilson, J. M. Byers, P. C. Dorsey, J. S. Horwitz, D. B. Chrisey, M. S. Osofsky., J. Appl. Phys. **81**, 4971 (1997).
[7] N. Cornei, M. -L. Craus, J. Optoelectron. Adv. Mater. **6**, 269 (2004).
[8] A. Boultif, A. Louer, J. Appl. Cryst. **24**, 987(1991).
[9] P. E. Werner, J. Appl.Cryst. **9**, 216 (1976).
[10] J, Laugier, B. Bochu, CheckCell, programme developpe dans Laboratoire de Physique de Grenoble (INPG).
[11] W. Kraus, G. Nolze, J. Appl. Cryst. **29**, 301 (1996).
[12] G. H. Jonker, Physica **22**, 707 (1956).
[13] T. Terai, T. Kakeshita, T. Fukuda, M.Yamamoto, T. Saburi, H. Kitagawa, K. Kindo, M. Honda, Trans. Mat. Res. Soc. Japan **25**, 217 (200).
[14] H. Kawano, R. Kajimoto, H. Yoshizawa,Y. Tomioka, H. Kuwahara, Y. Tokura, Cond-mat/9808286 (1998).
[15] T. Okuda, T. Kimura, Y. Tokura, Phys. Rev. **B60**, 3370 (1999).
[16] S. Yunoki, J. Hu, A. L. Malwezi, A. Moreo, N. Furukawa, E. Dagotto, Phys. Rev. Lett. **80**, 845 (1998).
[17] I. V. Solovyev, K. Terakura, Phys. Rev. **B63**, 174425 (2001).
[18] C. Ritter, R. Mahendiran, M. R. Ibarra, L. Morellon, A. Maignan, B. Raveau, C. N. R. Rao, Phys. Rev. **B61**, 9229 (2000).

*Coresponding author : kraus@nf.jinr.ru